Development of Dynamic EV Load Model for Power System Oscillatory Stability Studies

C.H. Dharmakeerthi*, N. Mithulananthan
School of ITEE, University of Queensland,
Brisbane, Australia.
*and Ceylon Electricity Board, Sri Lanka.
*p.dharmakeerthi@uq.edu.au, mithulan@itee.uq.edu.au.

A. Atputharajah,
Dept. of Electrical & Electronic Engineering
University of Peradeniya,
Sri Lanka.
atpu@ee.pdn.ac.lk.

***Abstract*— The interest on electric vehicles growing as a sustainable alternative to fossil fuel driven vehicles. Even though there are a number of grid impact studies, only a scant attention has been paid to study the impact of EV charging on system stability. Electrification of transportation brings significant load integration to the grid. This could profoundly influence stability of the grid. Hence, it is important to understand the EV charging impact on power system stability. The extant literature is largely based on conventional load characteristics rather than actual EV load behaviours, due to the unavailability of proper load models. Hence, this study develops a dynamic EV load model, considering the dynamics of the EV charger and the battery, as an essential basis for system oscillatory stability studies. Dynamic behavior of a power electronically controlled EV load is described by an eleventh order model. The preliminary results suggest that EV load can cause considerable influence on damping performance of electromechanical modes.**

***Index Terms*—Dynamic load model, Electric vehicle, oscillatory stability**

I. INTRODUCTION

Increasing concerns about global warming and fossil fuels dependencies have boost the interest on Electric Vehicles (EV). However, their integration into power grids brings additional challenges for the power system engineers worldwide. It is essential to evaluate the potential grid impacts of EV integration to guarantee secure grid operations.

A number of system studies have been undertaken by researchers on various issues related to EV grid integration so far. However, the literature survey in [1] has identified that the impact of EV charging on power system stability is not yet fully understood. The system load characteristics are among the main factors affecting system instabilities, mainly system voltage stability and oscillatory stability. However, accurate dynamic EV load models for system stability studies are yet to be developed. Hence, this paper discussed the development a dynamic models of an EV charging load for oscillatory stability studies.

The EV chargers can be categorised mainly into ac or dc chargers and further according to the power demand defined by the level of charging. The Level 1 charger is basically for home-based charging, while Level 3 chargers are commercial fast chargers. The level 2 charger could be either home-based or industrial depending on the power rating. The fast charger power rating can even exceed 200 kW [2] and the charging times falls within minutes scale. The time taken for fast charging is likely to be comparable to the average time taken for conventional vehicle refuelling. There is a high probability that fast charging will become popular as it appears to be a convenient charging option for EV users. Fast charging will place considerable demand on power networks and, hence, it is important to assess its impact on power systems.

The reliability of the outcomes of EV impact studies on power system stability is inevitably determined by the accuracy of the system modelling, including the load models incorporated to represent the EV load. However, different kinds of load models have been used in the literature to represent EV load behaviour in power systems studies. Among them, [3] has considered EV as a constant current load. On the other hand, [4] characterised EV as a constant power load and as a constant impedance load. These two studies were based on assumed load models rather than derived models. The studies in [5, 6] have derived static load models of EV fast charging load. The study in [7] has incorporated a derived static load model to evaluate the impact of EV charging load in system oscillatory stability. The probabilistic small signal stability study reported in [8] and the numerical small signal stability study found in [9] utilised dynamic models of single stage EV chargers in their evaluations. However, the modern high power chargers, which may have significant impact on system stability, consist of two stages (ac-dc and dc-dc) rather than having a simple single stage (ac-dc) structure. Hence, it is evident that the derivation of the system load models to represent the EV load for accurate stability studies is a primary task.

An EV fast charger, which consists of an active rectifier at the front-end and a dc-dc buck converter at the battery-end, is considered here for modelling the dynamic characteristics of an EV charging load, in Section II. Section III provides some

preliminary results of impact of EV charging on power system oscillatory stability, while Section IV presents the conclusions of the study.

II. Dynamic EV Load Model

The well-established EV charger configurations consist of two converters, namely an ac-dc converter at the front end and a dc-dc converter at the battery end [10-18], as shown in Fig.1. The first converter performs rectification and power factor control. This can be achieved either by incorporating an active rectifier or by using a rectifier together with a power factor correction circuit, as described in [19]. The second stage involves different types of resonant or pulse width modulated (PWM) dc-dc converters [18]. The dc-dc converter is required for maintaining an appropriate charging current for different SOC conditions and cell temperatures of the battery. Furthermore, the second converter stage maintains the charging current ripples within the safe limits of the battery [11, 20].

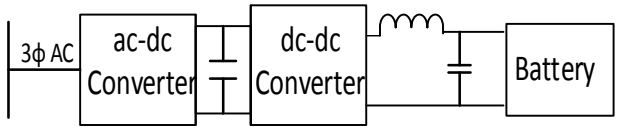

Fig.1 Schematic diagram of an EV charger.

Galvanic isolation between the power grid and the EV can be achieved by using high frequency transformers at the dc-dc stage or by using power frequency transformers at the grid interface [21]. High frequency isolation is preferred as it offers greatly reduced weight and size. Inductive charging can be achieved by separating the secondary winding of the isolation transformer and by placing them on board.

The analytical derivation of dynamic load model of an EV charging load is carried out in this section for oscillatory stability studies. The charger consists of essential elements shown in Fig. 2, namely an active rectifier, a buck converter, a battery units and the associated controllers.

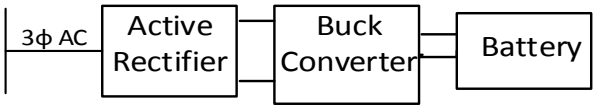

Fig. 2 A schematic diagram of an EV fast charger.

Dynamic modelling of the elements together with their controllers are presented in the proceeding section.

A. Modelling of ac-dc converter & controller

The derivation of the dynamic model of the ac-dc converter shown in Fig. 3 is carried out here.

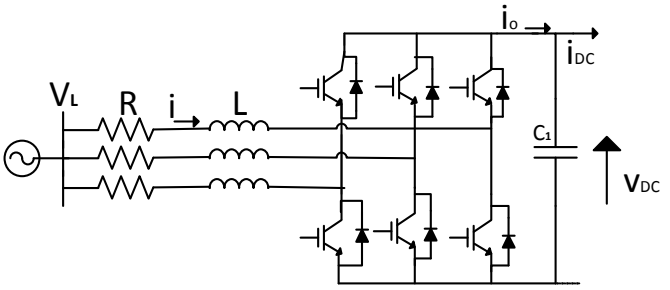

Fig. 3 A schematic diagram of an ac-dc converter.

A set of differential and algebraic equations is derived to describe the converter characteristics. In dq reference frame the ac-dc boost converter operation can be described as given below. The methodology involving in transforming abc reference frame quantities to dq reference frame can be found in [22].

$$L\frac{di_d}{dt} = v_d + \omega L i_q - d_d v_{DC} - R i_d \tag{1}$$

$$L\frac{di_q}{dt} = v_q - \omega L i_d - d_q v_{DC} - R i_q \tag{2}$$

$$C_1\frac{dv_{DC}}{dt} = \frac{3}{2}\left(d_d i_d + d_q i_q\right) - i_{DC} \tag{3}$$

It is assumed that the dq frame is rotating at ω speed and the d axis is oriented along the grid voltage vector. By selecting d axis along the grid voltage vector $V_L\angle\theta$,

$$v_d = V_L \tag{4}$$

$$v_q = 0 \tag{5}$$

The equations (1) and (2) can be rearranged as,

$$L\frac{di_d}{dt} = V_L + \omega L i_q - d_d v_{DC} - R i_d \tag{6}$$

$$L\frac{di_q}{dt} = -\omega L i_d - d_q v_{DC} - R i_q \tag{7}$$

The ac-dc converter controller shown in Fig. 4 is modelled next. The d axis current has been used to regulate the dc link voltage. The i_{qref} can be set to zero to achieve unity power factor operation.

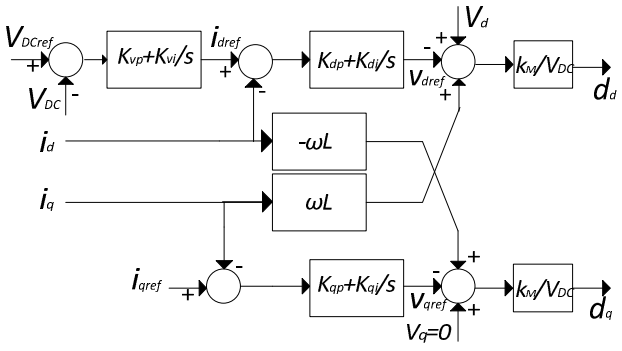

Fig. 4 A schematic diagram of the controller of the active rectifier.

A set of algebraic and differential equations which describes the converter characteristics can be derived as shown below.

The variables x_1, x_2 and x_3 are three added state variables to describe the ac-dc converter controller dynamic behaviour.

$$\frac{dx_1}{dt} = v_{DCref} - v_{DC} \tag{8}$$

$$i_{dref} = K_{vp}\left(v_{DCref} - v_{DC}\right) + K_{vi}x_1 \tag{9}$$

$$\frac{dx_2}{dt} = i_{dref} - i_d \tag{10}$$

$$v_{dref} = K_{dp}\left(i_{dref} - i_d\right) + K_{di}x_2 \tag{11}$$

$$d_d = \frac{k_M}{v_{DC}}\left(v_d - v_{dref} + \omega L i_q\right) \tag{12}$$

Solving (9) and (11),

$$v_{dref} = K_{dp}\left\{\left[K_{vp}\left(v_{DCref} - v_{DC}\right) + K_{vi}x_1\right] - i_d\right\} + K_{di}x_2 \tag{13}$$

Solving (12) and (13),

$$d_d = \frac{k_M}{v_{DC}}\left[v_d - K_{dp}\left\{K_{vp}\left(v_{DCref} - v_{DC}\right) + K_{vi}x_1 - i_d\right\} - K_{di}x_2 + \omega L i_q\right] \tag{14}$$

$$\frac{dx_3}{dt} = i_{qref} - i_q \tag{15}$$

$$v_{qref} = K_{qp}\left(i_{qref} - i_q\right) + K_{qi}x_3 \tag{16}$$

$$d_q = \frac{k_M}{v_{DC}}\left(v_q - v_{qref} - \omega L i_d\right) \tag{17}$$

Solving (16) and (17),

$$d_q = \frac{k_M}{v_{DC}}\left[v_q - K_{qp}\left(i_{qref} - i_q\right) - K_{qi}x_3 - \omega L i_d\right] \tag{18}$$

Modelling of dc-dc converter is considered next.

B. Modelling of dc-dc converter & controller

Analytical modelling of the second stage of the charger, which consists of a dc-dc converter, is considered here. The dc-dc converter and the controller are shown in Fig. 5.

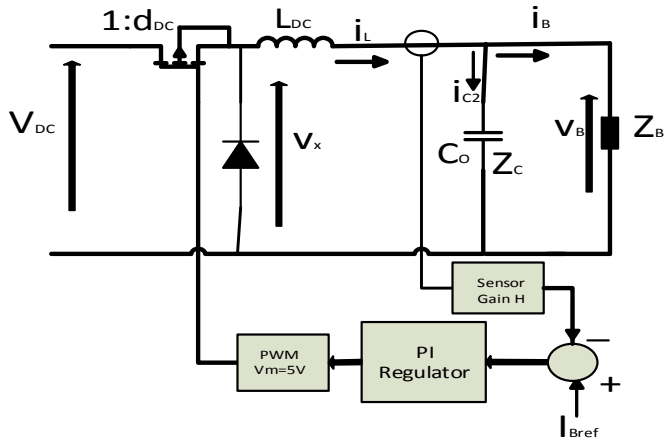

Fig. 5 A schematic diagram of dc-dc converter and its controller.

Lossless switching and continuous conduction mode operations of the buck converter are assumed. The battery charging current reference (I_{Bref}) is determined by the battery management system based on many factors, including the cell voltage and temperature. The effective series resistance of the current smoothing inductor is represented by r. The proportional and integral constant of the PI regulator are given by k_{pdc} and k_{idc}. Considering Fig. 4, the analytical expressions for the second stage can be derived as follow. The variable x_4 is an added state variable to describe dc-dc converter controller dynamics.

$$L_{dc}\frac{di_L}{dt} = d_{dc}v_{DC} - v_B - ri_L \tag{19}$$

$$C_2\frac{dv_B}{dt} = i_L - i_B \tag{20}$$

$$\frac{dx_4}{dt} = i_{Bref} - Hi_L \tag{21}$$

$$d_{dc} = \frac{K_{pdc}v_m}{i_L}\left(i_{Bref} - Hi_L\right) + \frac{K_{idc}x_4v_m}{i_L} \tag{22}$$

C. Modelling of the battery

Present day EV units use Nickel Metal Hydride (NiMH) or Lithium Ion (Li-ion) batteries. However, Li-ion battery technology will be more popular due to its higher specific energy (Wh/kg) and longer life span [23] [24]. The dynamic behaviour of the battery can be described as below.

Thermally dependent electrochemical reactions take place during charging or discharging of a battery. The properties of a battery change with the operation point, thus the battery parameters. Battery parameters depend on the SOC, operating temperature, extent of charging or discharging current, service life and others. Individual cells within a battery module are inherent with different characteristics even when they are new. Hence, precise battery modelling is challenging. Therefore, and reasonable assumptions can be made to reduce the model complexity depending on the application of the model. Higher order battery models which incorporate thermal, electrical and chemical properties of the battery can be utilised for battery management and condition monitoring applications. Whereas, system modelling for oscillatory stability studies, requires battery electrical status variations around an operating point when the power system undergoes small disturbances. Hence, it may be realistic to reduce the order of the battery model while not compromising its accuracy as described below.

Battery thermal model describes the effects of electrolytic temperature and ambient temperature variations on battery performance. However, the ambient temperature generally does not vary significantly within seconds to minutes time scale. Li-ion batteries incorporate advanced liquid cooling systems [23], while simple forced air cooling systems are employed in NiMH batteries. Hence, it is reasonable to assume the temperatures within the cells are maintained fairly constant during a small time period of few minutes. Based on that, it is practicable to consider the effects of electrolytic temperature variations on battery parameters are negligible during the considered time frame. Hence, the effects of battery thermal modal on the accuracy small signal stability studies will be of less significance and can be disregarded to reduce the complexity of the final battery model.

The values of battery parameters (internal resistances and capacitances) depend on battery SOC also. However, experiments demonstrate that the parameters remain fairly constant above a certain SOC range (typically above 10% of SOC) [25, 26], while the parameters change exponentially below that SOC. Mostly, EV recharging occurs well before the fully depletion of the battery for prolonged battery life. Hence, it is practicable to assume negligible variations to the internal resistances and capacitances considering the range of SOC and the time frame of the study, with respect to the modal application point of view [27].

A widely accepted battery model [25, 26, 28, 29] as shown in Fig. 6, is incorporated in this research. The two series connected parallel RC circuits define the transient characteristics of the battery, while R_{BO} describe charging/discharging power loss of the battery. V_{BO} is the battery open circuit voltage, which is a function of battery SOC. The battery electrochemical polarisation resistance and the capacitances are represented by R_{B1} and C_{B1} [26], respectively. The battery concentration polarisation resistance and the capacitances are represented by R_{B2} and C_{B2} [26].

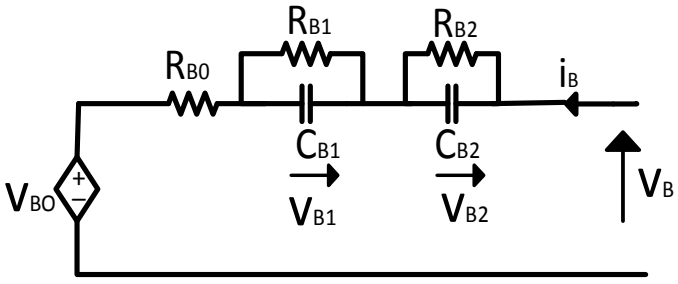

Fig. 6 The schematic diagram of battery.

The more the number of series connected parallel RC circuits, the more accurate is the model. However, it has been identified that two number of series connected parallel RC circuits will provide reasonably accurate dynamic performance with less computational complexities [29]. Hence, this research represents the battery with only two parallel RC units. The differential and algebraic equations describing the battery dynamics are shown below.

$$\frac{dv_{B1}}{dt} = \frac{1}{C_{B1}}\left(i_B - \frac{v_{B1}}{R_{B1}}\right) \tag{23}$$

$$\frac{dv_{B2}}{dt} = \frac{1}{C_{B2}}\left(i_B - \frac{v_{B2}}{R_{B2}}\right) \tag{24}$$

$$v_B = v_{BO} + i_B R_{BO} + v_{B1} + v_{B2} \tag{25}$$

The complete dynamic model of the EV charging load is shown in the next section.

D. EV dynamic load model

The EV dynamic load model can be obtained by considering the analysis from the Sections *A* to *C*. The EV dynamic load model can be described by an eleventh order model. The set of differential (26) and algebraic equations (27) are documented in Appendix. The mathematical model of EV charger dynamics given in (26) and (27) can be incorporated for evaluating the impact of EV load on power system oscillatory stability. Such a preliminary study is also carried out in this research as described in the proceeding section.

III. Impact of EV Charging on Oscillatory Stability

The dynamic model of the EV charging load developed in the Section II is incorporated to evaluate the impact on power system oscillatory stability. A modified SMIB with an additional load, as shown in Fig. 7, is considered in the analysis.

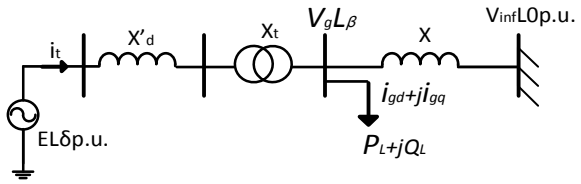

Fig. 7 Modified SMIB system.

The generator is modelled with the classical synchronous machine model, incorporating two ordinary differential equations. The data associated with the system and the EV load are given in the Appendix. Impact of EV charging load on system oscillatory stability is evaluated by Eigenvalue analysis of the system state matrix. The Eigenvalues and the most associated state variables are shown in TABLE I.

TABLE I
The Eigenvalues and the most associated state variables

Mode No.	Eigenvalues	Most associated state variables
1	-13.2 x e^6	i_{gq}
2	-5.0 x e^6	i_{gd}
3	-3.9 x e^5	i_L
4	-6.6 x e^4	v_b
5	-76.1	x_2, x_3
6	-72.7	x_2, x_3
7	-0.86 + 6.33i	δ, ω
8	-0.86 - 6.33i	δ, ω
9	-0.34+ 4.36i	v_{dc}, x_1
10	-0.34- 4.36i	v_{dc}, x_1
11	-0.19	v_{B1}
12	-0.09	x_4
13	-0.017	v_{B2}

The test system with EV charging load is stable, as all the Eigenvalues (modes) have negative real parts. There are two complex (oscillatory) modes. One oscillatory mode (7 and 8) is due to electro-mechanical oscillation associated with the generator rotor angle and speed state variables. The other oscillatory mode (9 and 10) is mostly contributed by the state variables v_{dc} and x_1, which are associated with dc link capacitor voltage and the ac-dc converter controller, respectively. The modes 11-13 are having lowest negative real parts and mostly contributed by v_{B1}, x_4 and v_{B2} state variables, respectively. Hence, properly tuned dc-dc converter controller may minimise the impact of these modes, as these state variables are associated with the battery and the dc-dc converter control system.

Further, the influence of resistance R (which comprises of the parasitic resistance of input filter inductor, the on-state resistance of the ac-dc converter switches and the lead

conductor resistances) on system oscillatory modes (modes 7-10) is evaluated. The results are shown in the TABLE II.

TABLE II
THE EIGENVALUES AND THE MOST ASSOCIATED STATE VARIABLES

Modes	R=0.1 mΩ	R=1 mΩ	R=10 mΩ	R=20 mΩ
7,8	-0.8651 ± 6.3331i	-0.8649 ± 6.3332i	-0.8633 ± 6.3349i	-0.8616 ± 6.3368i
9,10	-0.3453 ± 4.3649i	-0.3454 ± 4.3626i	-0.3459 ± 4.3402i	-0.3464 ± 4.3152i

It is evident from the results that the modes associated with the dc link voltage and the ac-dc converter controller (x_1) improve when the resistance is increased, while the electro-mechanical modes are deteriorated. The results also in agreement with study outcomes reported in [30], which reports that higher R values cause higher negative impact on system electromechanical modes.

IV. CONCLUSIONS

A dynamic model of the EV load has been derived by considering the dynamic characteristics of the EV charger and the battery. This includes the detail modelling of the charger ac-dc converter, dc-dc converter, battery unit and the converter controllers. Model development captured all the dominated dynamics of the EV charging load in system oscillatory stability studies perspective, while approximating the less apparent dynamics to reduce model complexity. The dynamics of EV charging load could be best described by an eleventh order model. The developed EV load model could be efficiently incorporated in system oscillatory stability studies to identify the impacts of EV fast charging on power system low frequency oscillations. The preliminary oscillatory stability study found that EV charging load cause considerable influence on the system electromechanical modes. Further, increasing values of resistance R (which comprises of the parasitic resistance of input filter inductor, the on-state resistance of the ac-dc converter switches and resistance of the lead conductor/cable) increased the negative impacts of EV charging on the system oscillatory modes.

V. APPENDIX

$$\begin{bmatrix} \dot{i}_d \\ \dot{i}_q \\ \dot{v}_{DC} \\ \dot{x}_1 \\ \dot{x}_2 \\ \dot{x}_3 \\ \dot{i}_L \\ \dot{V}_B \\ \dot{x}_4 \\ \dot{v}_{B1} \\ \dot{v}_{B2} \\ \end{bmatrix} = \begin{bmatrix} -R/L & \omega & -d_d/L & 0 & 0 & 0 & 0 & 0 & 0 & 0 & 0 & 0 \\ -\omega & -R/L & -d_q/L & 0 & 0 & 0 & 0 & 0 & 0 & 0 & 0 & 0 \\ 3d_d/2C_1 & 3d_q/2C_1 & 0 & 0 & 0 & 0 & 0 & 0 & 0 & 0 & 0 & 0 \\ 0 & 0 & -1 & 0 & 0 & 0 & 0 & 0 & 0 & 0 & 0 & 0 \\ -1 & 0 & 0 & 0 & 0 & 0 & 0 & 0 & 0 & 0 & 0 & 0 \\ 0 & -1 & 0 & 0 & 0 & 0 & 0 & 0 & 0 & 0 & 0 & 0 \\ 0 & 0 & d_{dc}/L_{dc} & 0 & 0 & 0 & -r/L_{dc} & -1/L_{dc} & 0 & 0 & 0 & 0 \\ 0 & 0 & 0 & 0 & 0 & 0 & 1/C_2 & 0 & 0 & 0 & 0 & 0 \\ 0 & 0 & 0 & 0 & 0 & 0 & -H & 0 & 0 & 0 & 0 & 0 \\ 0 & 0 & 0 & 0 & 0 & 0 & 0 & 0 & 0 & -1/R_{B1}C_{B1} & 0 & 0 \\ 0 & 0 & 0 & 0 & 0 & 0 & 0 & 0 & 0 & 0 & -1/R_{B2}C_{B2} & 0 \end{bmatrix} \begin{bmatrix} i_d \\ i_q \\ v_{DC} \\ x_1 \\ x_2 \\ x_3 \\ i_L \\ V_B \\ x_4 \\ v_{B1} \\ v_{B2} \\ \end{bmatrix} + \begin{bmatrix} V_L/L \\ 0 \\ -i_{DC} \\ v_{DCref} \\ i_{dref} \\ i_{qref} \\ 0 \\ -i_B/C_2 \\ i_{Bref} \\ i_B/C_{B1} \\ i_B/C_{B2} \\ \end{bmatrix} \quad (26)$$

$$[0] = \begin{bmatrix} 0 & 0 & -K_{vp} & K_{vi} & 0 & 0 & 0 & 0 & 0 & 0 & 0 \\ -K_{dp} & 0 & -K_{vp}K_{dp} & K_{dp}K_{vi} & K_{di} & 0 & 0 & 0 & 0 & 0 & 0 \\ K_{dp} & \omega L & -d_d/k_M + K_{vp}K_{dp} & -K_{dp}K_{vi} & -K_{di} & 0 & 0 & 0 & 0 & 0 & 0 \\ 0 & -K_{qp} & 0 & 0 & 0 & +K_{qi} & 0 & 0 & 0 & 0 & 0 \\ -\omega L & K_{qp} & -d_q/k_M & 0 & 0 & -K_{qi} & 0 & 0 & 0 & 0 & 0 \\ 0 & 0 & 0 & 0 & 0 & 0 & -K_{pdc}H/v_m & 0 & K_{idc}/v_m & 0 & 0 \\ 0 & 0 & 0 & 0 & 0 & 0 & 0 & -1 & 0 & 1 & 1 \end{bmatrix} \begin{bmatrix} i_d \\ i_q \\ v_{DC} \\ x_1 \\ x_2 \\ x_3 \\ i_L \\ V_B \\ x_4 \\ v_{B1} \\ v_{B2} \\ \end{bmatrix} + \begin{bmatrix} -i_{dref} + K_{vp}v_{DCref} \\ -v_{dref} + K_{vp}K_{dp}v_{DCref} \\ V_L - K_{vp}K_{dp}v_{DCref} \\ K_{qp}i_{qref} - v_{qref} \\ -K_{qp}i_{qref} \\ K_{pdc}i_{Bref}/v_m - D \\ i_B R_{BO} + v_{B0} \\ \end{bmatrix} \quad (27)$$

The system and EV load parameter values incorporated in Eigenvalue analysis in Section III, are given below in TABLE III.

TABLE III
THE SYSTEM AND EV DATA

Parameter	Value
C_2	360μF
L	20μH
ω	377 $rads^{-1}$
R	0.1 mΩ
C_{B1}	300F
K_d	10
i_L	200A
βo	15°
V_m	5
R_{B1}	0.0437 Ω
V_{inf}	0.995 p.u.
X_d'	0.2 p.u.
r	1.0 mΩ
X_t	0.1 p.u.
X_1	0.5 p.u.
V_{dco}	650 V
C_{B2}	5088F
H_g	3.5
v_{BO}	384.5V
v_g	1.0 p.u.
R_{B0}	0.1053
R_{B2}	0.0288
k_M	392
L_{dc}	60μH

VI. REFERENCES

[1] C.H.Dharmakeerthi, N.Mithulananthan , and T.K.Saha, "Overview of the Impacts of Plug-in Electric Vehicles on the Power Grid," in *Innovative Smart Grid Technologies (ISGT) Asia Conference*, Perth, 2011.

[2] SAE. Charging configurations and Ratings Terminology-SAE Hybrid Committee [Online].

[3] M. El Chehaly, O. Saadeh, C. Martinez, and G. Joos, "Advantages and applications of vehicle to grid mode of operation in plug-in hybrid electric vehicles," in *Electrical Power & Energy Conference (EPEC), 2009 IEEE*, 2009, pp. 1-6.

[4] T. Das and D. C. Aliprantis, "Small-Signal Stability Analysis of Power System Integrated with PHEVs," in *Energy 2030 Conference, 2008. ENERGY 2008. IEEE*, 2008, pp. 1-4.

[5] C. H. Dharmakeerthi, N. Mithulananthan, and T. K. Saha, "Modeling and planning of EV fast charging station in power grid," in *Power and Energy Society General Meeting, 2012 IEEE*, 2012, pp. 1-8.

[6] C. H. Dharmakeerthi, N. Mithulananthan, and T. K. Saha, "Impact of electric vehicle fast charging on power system voltage stability," *International Journal of Electrical Power & Energy Systems,* vol. 57, pp. 241-249, 2014.

[7] C. H. Dharmakeerthi, N. Mithulananthan, and T. K. Saha, "Impact of electric vehicle load on power system oscillatory stability," in *Power Engineering Conference (AUPEC), 2013 Australasian Universities*, 2013, pp. 1-6.

[8] H. Huang, C. Y. Chung, K. W. Chan, and H. Chen, "Quasi-Monte Carlo Based Probabilistic Small Signal Stability Analysis for Power Systems With Plug-In Electric Vehicle and Wind Power Integration," *Power Systems, IEEE Transactions on,* vol. PP, pp. 1-9, 2013.

[9] F. R. Islam, H. R. Pota, M. A. Mahmud, and M. J. Hossain, "Impact of PHEV loads on the dynamic performance of power system," in *Universities Power Engineering Conference (AUPEC), 2010 20th Australasian*, 2010, pp. 1-5.

[10] R. M. Miskiewicz, A. J. Moradewicz, and M. P. Kazmierkowski, "Contactless battery charger with bi-directional energy transfer for plug-in vehicles with vehicle-to-grid capability," in *Industrial Electronics (ISIE), 2011 IEEE International Symposium on*, 2011, pp. 1969-1973.

[11] B. Bilgin, A. Emadi, and M. Krishnamurthy, "Design considerations for a universal input battery charger circuit for PHEV applications," in *Industrial Electronics (ISIE), 2010 IEEE International Symposium on*, 2010, pp. 3407-3412.

[12] D. Gautam, F. Musavi, M. Edington, W. Eberle, and W. G. Dunford, "An automotive on-board 3.3 kW battery charger for PHEV application," in *Vehicle Power and Propulsion Conference (VPPC), 2011 IEEE*, 2011, pp. 1-6.

[13] S. Dusmez, A. Cook, and A. Khaligh, "Comprehensive analysis of high quality power converters for level 3 off-board chargers," in *Vehicle Power and Propulsion Conference (VPPC), 2011 IEEE*, 2011, pp. 1-10.

[14] A. Kuperman, U. Levy, J. Goren, A. Zafranski, A. Savernin, and I. Peled, "Modeling and control of a 50KW electric vehicle fast charger," in *Electrical and Electronics Engineers in Israel (IEEEI), 2010 IEEE 26th Convention of*, 2010, pp. 000188-000192.

[15] S. Jaganathan and G. Wenzhong, "Battery charging power electronics converter and control for plug-in hybrid electric vehicle," in *Vehicle Power and Propulsion Conference, 2009. VPPC '09. IEEE*, 2009, pp. 440-447.

[16] L. Young-Joo, A. Khaligh, and A. Emadi, "Advanced Integrated Bidirectional AC/DC and DC/DC Converter for Plug-In Hybrid Electric Vehicles," *Vehicular Technology, IEEE Transactions on,* vol. 58, pp. 3970-3980, 2009.

[17] X. P. Yan, DJ "A High Efficiency On-Board Battery Charger with Unity Input Power Factor " presented at the Australasian Universities Power Engineering Conference Darwin 1999

[18] M. G. Egan, D. L. O'Sullivan, J. G. Hayes, M. J. Willers, and C. P. Henze, "Power-Factor-Corrected Single-Stage Inductive Charger for Electric Vehicle Batteries," *Industrial Electronics, IEEE Transactions on,* vol. 54, pp. 1217-1226, 2007.

[19] A. Kuperman, U. Levy, J. Goren, A. Zafranski, A. Savernin, and I. Peled, "Modeling and control of a 50KW electric vehicle fast charger," in *Electrical and Electronics Engineers in Israel (IEEEI), 2010 IEEE 26th Convention of*, pp. 000188-000192.

[20] B. Bilgin, E. Dal Santo, and M. Krishnamurthy, "Universal input battery charger circuit for PHEV applications with simplified controller," in *Applied Power Electronics Conference and Exposition (APEC), 2011 Twenty-Sixth Annual IEEE*, pp. 815-820.

[21] A. M. Chris Mi, David Wenzhong Gao. (2011, 26/09/11). *Hybrid electric vehicles [electronic resource] : principles and applications with practical perspectives*

[22] C. Schauder and H. Mehta, "Vector analysis and control of advanced static VAr compensators," *Generation, Transmission and Distribution, IEE Proceedings C,* vol. 140, pp. 299-306, 1993.

[23] K. Young, C. Wang, L. Wang, and K. Strunz, "Electric Vehicle Battery Technologies," in *Electric Vehicle Integration into Modern Power Networks*, R. Garcia-Valle and J. A. Peças Lopes, Eds., ed: Springer New York, 2013, pp. 15-56.

[24] G. Lijun, S. Liu, and R. A. Dougal, "Dynamic lithium-ion battery model for system simulation," *Components and Packaging Technologies, IEEE Transactions on,* vol. 25, pp. 495-505, 2002.

[25] C. Min and G. A. Rincon-Mora, "Accurate electrical battery model capable of predicting runtime and I-V performance," *Energy Conversion, IEEE Transactions on,* vol. 21, pp. 504-511, 2006.

[26] H. Hongwen, X. Rui, Z. Xiaowei, S. Fengchun, and F. JinXin, "State-of-Charge Estimation of the Lithium-Ion Battery Using an Adaptive Extended Kalman Filter Based on an Improved Thevenin Model," *Vehicular Technology, IEEE Transactions on,* vol. 60, pp. 1461-1469, 2011.

[27] D. Fregosi, S. Bhattacharya, and S. Atcitty, "Empirical battery model characterizing a utility-scale carbon-enhanced VRLA battery," in *Energy Conversion Congress and Exposition (ECCE), 2011 IEEE*, 2011, pp. 3541-3548.

[28] K. Taesic and Q. Wei, "A Hybrid Battery Model Capable of Capturing Dynamic Circuit Characteristics and Nonlinear Capacity Effects,"

Energy Conversion, IEEE Transactions on, vol. 26, pp. 1172-1180, 2011.

[29] Z. Hanlei and C. Mo-Yuen, "Comprehensive dynamic battery modeling for PHEV applications," in *Power and Energy Society General Meeting, 2010 IEEE*, 2010, pp. 1-6.

[30] C. H. Dharmakeerthi and N. Mithulananthan, "A study of load and line characteristics on power system damping performance," in *Industrial and Information Systems (ICIIS), 2013 8th IEEE International Conference on*, 2013, pp. 6-11.